Structural basis for the interaction between human milk oligosaccharides and the bacterial lectin PA-IIL of *Pseudomonas aeruginosa*

Stéphanie PERRET*[1], Charles SABIN*†[1], Claire DUMON*, Martina POKORNÁ‡, Catherine GAUTIER*, Oxana GALANINA§, Shahov ILIA§, Nicolai BOVIN§, Magali NICAISE‖, Michel DESMADRIL‖, Nechama GILBOA-GARBER¶, Michaela WIMMEROVÁ‡, Edward P. MITCHELL† and Anne IMBERTY*[2]

*Centre de Recherches sur les Macromolécules Végétales, CNRS (affiliated with Université Joseph Fourier), BP53, 38041 Grenoble Cedex 09, France, †E.S.R.F. Experiments Division, BP 220, F-38043, Grenoble Cedex, France, ‡National Centre for Biomolecular Research and Department of Biochemistry, Masaryk University, Kotlarska 2, 611 37 Brno, Czech Republic, §Shemyakin & Ovchinnikov Institute of Bioorganic Chemistry, Russian Academy of Sciences ul Miklukho-Maklaya 16/10, 17871 GSP-7, V-437, Moscow, ‖UMR 8619 – IBBMC, Modélisation et Ingénierie des Protéines, Bât. 430 Université Paris XI, 91405 Orsay, France, and ¶Bar-Ilan University, Faculty of Life Sciences, Ramat Gan 52900, Israel

One of the mechanisms contributing to the protection by breast-feeding of the newborn against enteric diseases is related to the ability of human milk oligosaccharides to prevent the attachment of pathogenic bacteria to the duodenual epithelium. Indeed, a variety of fucosylated oligosaccharides, specific to human milk, form part of the innate immune system. In the present study, we demonstrate the specific blocking of PA-IIL, a fucose-binding lectin of the human pathogen *Pseudomonas aeruginosa*, by milk oligosaccharides. Two fucosylated epitopes, Lewis a and 3-fucosyl-lactose (Lewis x glucose analogue) bind to the lectin with dissociation constants of 2.2×10^{-7} M and 3.6×10^{-7} M respectively. Thermodynamic studies indicate that these interactions are dominated by enthalpy. The entropy contribution is slightly favourable when binding to fucose and to the highest-affinity ligand, Lewis a. The high-resolution X-ray structures of two complexes of PA-IIL with milk oligosaccharides allow the precise determination of the conformation of a trisaccharide and a pentasaccharide. The different types of interaction between the oligosaccharides and the protein involve not only hydrogen bonding, but also calcium- and water-bridged contacts, allowing a rationalization of the thermodynamic data. This study provides important structural information about compounds that could be of general application in new therapeutic strategies against bacterial infections.

Key words: crystal structure, fucose, human milk oligosaccharide, lectin, *Pseudomonas aeruginosa*, thermodynamics.

INTRODUCTION

Pseudomonas aeruginosa is an opportunistic pathogen that infects immunosuppressed individuals and compromised tissues, such as burn wounds or the trachea of intubated patients. The bacteria endanger especially patients with cystic fibrosis. For pathogenic organisms, the ability to adhere to host tissues is essential to initiate an infection, and host cell surface glycoconjugates represent a specific target for bacterial receptors [1]. *P. aeruginosa* produces a variety of carbohydrate-binding proteins that could be involved in host recognition and adhesion. Some of them are located at the tip of pili [2] and flagella [3], whereas others are soluble lectins present in the cytoplasm and at the surface of the bacteria [4].

The role of carbohydrate–lectin adhesion in several bacterial infections of the stomach, ears and bladder has been recognized, and oligosaccharide-based treatments have been tried [5,6]. In the intestine of the human newborn, maternal milk oligosaccharides offer natural protection against pathogen infection [7]. Human milk contains a significant amount of structurally diverse oligosaccharides, most of which are fucosylated neutral oligosaccharides carrying lactose at their reducing end [8] (Figure 1). Since human milk oligosaccharides are soluble analogues of epithelial cell surface glycoconjugates, they competitively inhibit the binding of pathogenic bacteria and viruses to epithelial ligands [9]. More particularly, fucosylated human milk oligosaccharides inhibit binding *in vitro* or *in vivo* of several pathogens, such as entero-

pathic *Escherichia coli* [10], *Campylobacter jejuni* [11], Norwald-like virus [12] and *Helicobacter pylori* [13]. *P. aeruginosa* can also colonize the gastrointestinal tract and cause paediatric diarrhoea. Moreover, undetected endogenous gastrointestinal carriage can lead to severe infection in other parts of the body [14,15].

A fucose-binding lectin, PA-IIL, has been isolated from the *P. aeruginosa* cytoplasm [4] and its amino acid sequence characterized [16]. This soluble lectin is also present at the surface of the bacterial cell [17], is regulated by quorum sensing and is associated with virulence factors [18]. It has been demonstrated recently that human milk, but not cow's milk, specifically blocks haemagglutination by PA-IIL [19]. In the last 2 years, our group has deciphered the structural basis of the interaction between PA-IIL and fucose [20,21]. Fucose binding is mediated by two calcium ions, and this very unusual binding mode is responsible for the affinity (K_a 0.18×10^6 M^{-1}), which is much higher than is classically observed in protein–carbohydrate interactions [22].

Characterization of the interaction between PA-IIL and human milk oligosaccharides may help in understanding the role of PA-IIL in bacterial infection. Furthermore, detailed description of the structural and thermodynamic interactions will help in the design of carbohydrate-based compounds that can be used against *P. aeruginosa* infections such as those that threaten the lives of cystic fibrosis patients. We present here a study of the fine specificity of PA-IIL towards a number of human milk oligosaccharides, and characterization of the thermodynamics of binding
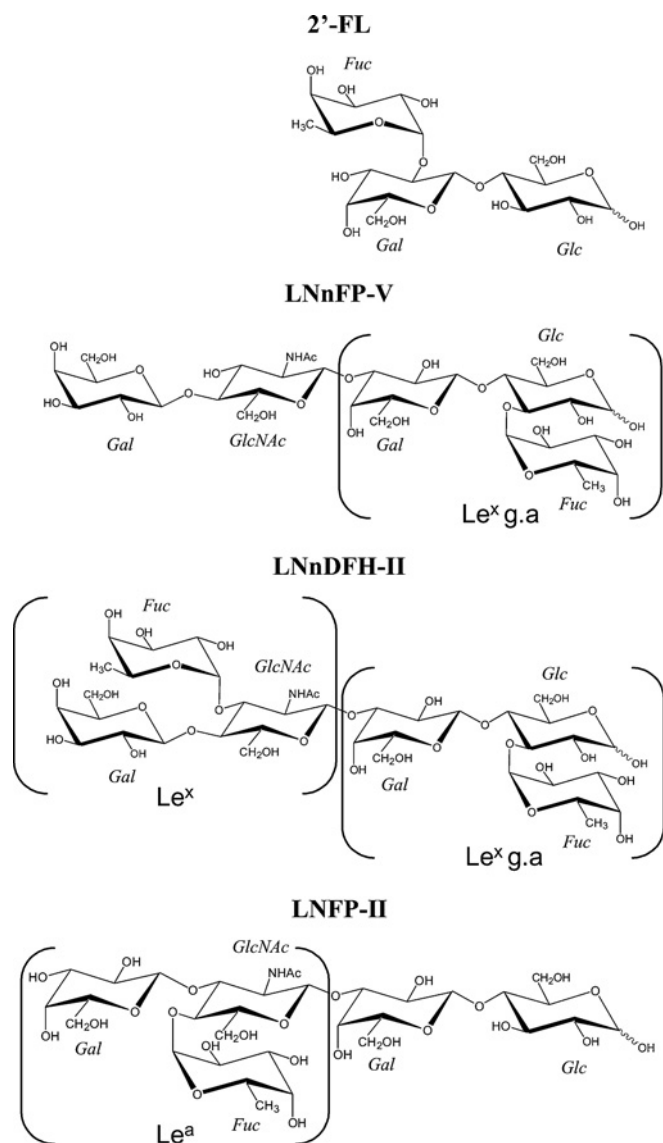
Figure 1   Representation of major human milk oligosaccharides illustrating the great variety of neutral oligosaccharide structures

All core molecules carry lactose at their reducing end. 2′-FL, 2′-FucLac. Lewis structures are shown in brackets.

for the highest-affinity ligand. The crystal structures of PA-IIL in complex with fucosylated tri- and penta-saccharide have been solved to a resolution of 1.75 and 1.05 Å respectively (where 1 Å = 0.1 nm), yielding the first atomic-resolution structures of human milk oligosaccharides and their interaction with bacterial receptors.

MATERIALS AND METHODS

Materials

Recombinant PA-IIL was purified from *Escherichia coli* BL21(DE3) containing the plasmid pET25pa2l as described previously [21]. L-Fuc and 2′-FucLac (2′-fucosyl-lactose) were purchased from Sigma; Me-αFuc (methyl-α-L-fucopyranoside) was purchased from Interchim; LNFP-II (lacto-*N*-fucopentaose II), Le^x (Lewis x), Le^a (Lewis a), SiaLe^a (sialyl Lewis a) and SiaLe^x (sialyl Lewis x) were purchased from Dextra. 3-FucLac,

LNnFP-V (lacto-*N*-neofucopentaose-V) and LNnDFH-II (lacto-*N*-neodifucohexaose-II) were produced in engineered *E. coli* strains and purified as described previously [23].

ELLA (enzyme-linked lectin assay) experiments

ELLAs were conducted using 96-well microtitre plates (Nunc Maxisorb) coated with PA-IIL (5 μg/ml) diluted in carbonate buffer, pH 9.6 (100 μl) for 1 h at 37 °C. After blocking at 37 °C for 1 h with 100 μl per well of 3 % (w/v) BSA in PBS, plates were incubated at 37 °C for 1 h with 100 μl of biotinylated polymeric fucose (Lectinity Holding, Inc.) at 5 μg/ml in the presence of serial dilutions of inhibitors. After washing with T-PBS (PBS containing 0.05 % Tween), 100 μl of streptavidin–peroxidase conjugate (dilution 1:5000; Boehringer-Mannheim) was added and left for 1 h at 37 °C. The colour was developed using 100 μl per well of 0.05 M phosphate/citrate buffer containing *O*-phenylenediamine dihydrochloride (0.4 mg/ml) and urea hydrogen peroxide (0.4 mg/ml) (Sigma-Aldrich). The reaction was stopped by the addition of 50 μl of 30 % H_2SO_4. Absorbance was read at 490 nm using a microtitre plate reader (Bio-Rad; model 680).

ITC (isothermal titration microcalorimetry) analysis

ITC experiments were performed with a VP-ITC isothermal titration calorimeter (Microcal). The experiments were carried out at 25 °C. Sugars and proteins were dissolved in the same buffer, i.e. 0.1 M Tris with 0.03 mM $CaCl_2$ at pH 7.5. The protein concentration in the microcalorimeter cell (1.4 ml) varied from 23.5 to 50 μM. A total of 22 injections of 13 μl of sugar solution at concentrations varying from 0.24 to 0.5 mM were added at intervals of 5 min while stirring at 310 rev./min. Control experiments performed by injection of buffer into the protein solution yielded insignificant heats of dilution. The experimental data were fitted to a theoretical titration curve using software supplied by Microcal, with ΔH (enthalpy change), K_a (association constant) and n (number of binding sites per monomer) as adjustable parameters, from the relationship:

$$Q_i = \frac{nP_t\Delta H V_o}{2}\left[1 + \frac{A_t}{nP_t} + \frac{1}{nKP_t}\right.$$
$$\left. - \sqrt{\left(1 + \frac{A_t}{nP_t} + \frac{1}{nKP_t}\right)^2 - 4\frac{A_t}{nP_t}}\right]$$

where P_t is the total protein concentration, A_t is the total concentration of the ligand, V_o is the volume of the cell and Q_i is the total heat released for injection i. ΔG values and entropy contributions were determined from the standard equation:

$$\Delta G = -RT \ln K = \Delta H - T\Delta S$$

where ΔG, ΔH and ΔS are the changes in free energy, enthalpy and entropy respectively of binding, T is the absolute temperature, $R = 8.32$ J · mol^{-1} · K^{-1} and K is the association constant. All experiments were performed with c values $100 < c < 200$ ($c = K_a M$, where M is the initial concentration of the macromolecule).

Crystallization

Crystallization conditions were screened using the hanging-drop vapour diffusion method from complete Hampton Screens I and II (Hampton Research) and the best conditions were selected. For the PA-IIL–LNnFP-V complex, hanging drops were prepared using 2.5 μl of lyophilized purified PA-IIL dissolved in water (10 mg · ml^{-1}) in the presence of LNnFP-V (1300 μg · ml^{-1}) and

CaCl$_2$ salt (2 mM) and 2.5 μl of reservoir solution (1.75 M ammonium sulphate in 0.1 M Tris/HCl, pH 8.5). Crystals, obtained within 3 weeks at 20°C, belong to space group P1 ($a = 47.01$ Å, $b = 48.35$ Å, $c = 52.47$ Å, $\alpha = 85.35°$, $\beta = 80.05°$ and $\gamma = 65.60°$), with four molecules per asymmetric unit, corresponding to a V_m (Matthews coefficient) of 2.3 Å$^3 \cdot$ Da^{-1} and a solvent content of 46 %. For the PA-IIL–Le^a complex, lyophilized protein was dissolved in water (10 mg $\cdot$ ml^{-1}) in the presence of Le^a (806 μg $\cdot$ ml^{-1}) and CaCl$_2$ salt (2 mM). Crystalline plates were obtained from hanging drops of 2.5 μl of protein solution mixed with 2.5 μl of reservoir solution {0.1 M sodium cacodylate at pH 6.5, 30 % PEG [poly(ethylene glycol)] 8000 and 0.2 M ammonium sulphate}. The crystal plates belong to space group P2$_1$ ($a = 51.57$ Å, $b = 75.82$ Å, $c = 52.74$ Å and $\beta = 93.48°$), with four molecules per asymmetric unit, resulting in a V_m of 2.2 Å$^3 \cdot$ Da^{-1} and a solvent content of 44 %.

Data collection and structure solution

Crystals were cryo-cooled at 100 K after soaking them for as short a time as possible in 25 % (v/v) glycerol in the precipitant solution. All data images were recorded on an ADSC Q4R CCD detector (Quantum Corp.) at a wavelength of 0.934 Å on beamline ID14-1 at ESRF (Grenoble, France). Data were processed with MOSFLM [24], and scaled and converted to structure factors using the CCP4 programme suite [25]. In the particular case of the 1.05 Å PA-IIL–LNnFP-V complex, to avoid the loss of the strongest reflections owing to saturation, three sets of data (one low- and two high-resolution passes) were collected from the same crystal.

Phasing of the PA-IIL–LNnFP-V complex was performed with ACORN [26], using only the positions of three of the calcium ions from the crystal structure of the PA-IIL–fucose complex solved previously at 1.0 Å resolution [21]. Using the ACORN phases, an initial structure was built automatically using ARP/warp [27]. The resulting electron density maps showed clear features corresponding to the oligosaccharide ligands. Cycles of iterative manual rebuilding and refinement were performed using the programs O [28] and REFMAC [29]. In the binding sites of monomers A and C, only four and three sugar residues respectively could be positioned in the electron density maps, whereas a pentasaccharide could be positioned in monomers B and D.

The structure of the Le^a-complexed lectin was solved by the molecular replacement technique with the MOLREP program [25], using the monomeric structure of the PA-IIL–fucose complex (PDB code 1GZT) stripped of water molecules and calcium ions as the search probe. Four clear solutions were found, corresponding to a tetramer in the asymmetric cell described previously [20]. The initial F_o–F_c difference maps showed clearly the presence of four Le^a ligands, one for each monomer. Cycles of manual model rebuilding with O and refinement with REFMAC gave the final structure. Co-ordinates of the final structures (see refinement statistics in Table 1) have been deposited in the Protein Data Bank under codes 1W8F and 1W8H for the LNnFP-V- and Le^a-complexed structures respectively.

RESULTS

Specificity of the interaction between PA-IIL and human milk oligosaccharides

Since haemagglutination by PA-IIL has been demonstrated to be blocked specifically by human milk [19], we studied the affinity of different human milk oligosaccharides towards the lectin using ELLAs. The fucosylated oligosaccharides shown in Figure 1 were tested for their inhibitory properties against the binding

Table 1 Data collection and refinement statistics

Data in parentheses show statistics for the highest-resolution shell. rmsd, root mean square deviation.

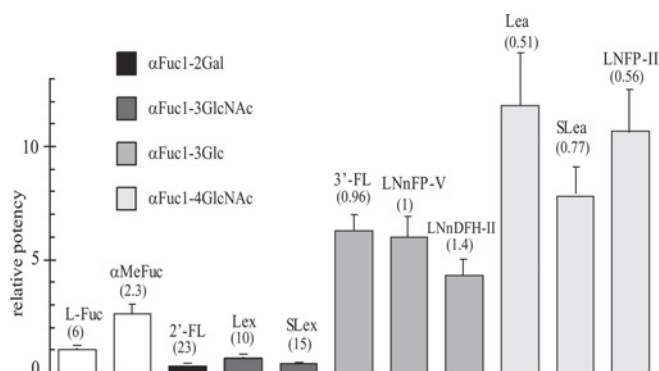| Parameter	PA-IIL–LNnFP-V	PA-IIL–Le^a
Data collection		
Wavelength (Å)	0.934	0.934
Resolution (Å)	14.51–1.05 (1.08–1.05)	26.82–1.75 (1.81–1.75)
Space group	P1	P2$_1$
Unit cell	$a = 47.015$ Å, $b = 48.352$ Å, $c = 52.472$ Å, $\alpha = 85.35°$, $\beta = 80.05°$, $\gamma = 65.60°$	$a = 51.57$ Å, $b = 75.82$ Å, $c = 52.74$ Å, $\beta = 93.48°$
Observed reflections	737 998	141 130
Unique reflections	180 478	34 767
Multiplicity	4.1 (3.5)	4.1 (3.4)
Completeness (%)	93.3 (89.5)	85.7 (41.7)
$I/\sigma I$	7.0 (1.8)	13.2 (3.8)
R_{merge} (%)	6.6 (32.2)	8.8 (33.0)
Refinement statistics		
R_{cryst} (%) (no. reflections)	10.5 (171 406)	12.5 (34 037)
R_{free} (%) (no. reflections)	12.3 (9072)	16.9 (730)
Average B factor (Å^2)	7.314	9.679
Protein atoms (n)	3564	3362
Ligand/water atoms (n)	197/727	204/438
rmsd bonds (Å)	0.021	0.014
rmsd angles (°)	2.1	1.5

Figure 2 Potency of different sugars relative to fucose

IC$_{50}$ values in μM, as determined from the inhibition curves, are given in parentheses. Each value has been averaged from at least three independent measurements. FL, FucLac; SLe, SiaLe.

of L-fucose-biotinylated polyacrylamide to immobilized PA-IIL. These oligosaccharides are representative of the variety of fucosylated epitopes found in human milk oligosaccharides: αFuc1-2Gal, αFuc1-4GlcNAc, αFuc1-3GlcNac and αFuc1-3Glc. IC$_{50}$ values ranged from 23 μM for 2'-FucLac to 0.5 μM for the best inhibitor, Le^a. After normalizing values to that of fucose, the inhibitory potency of the oligosaccharides appears to be directly dependent on the linkage between the fucose moiety and the carrying oligosaccharides (Figure 2). Oligosaccharides containing a fucose residue linked to position 2 of galactose (2'-FucLac) are poor inhibitors. Similarly, the Le^x series, which contain a fucose on position 3 of a GlcNAc residue, bind less efficiently to PA-IIL than does fucose alone. On the other hand, the Le^x g.a. (Le^x glucose analogue) series, in which the GlcNAc is replaced by Glc, binds approx. 6-fold better than fucose. The best inhibitors belong to the Le^a series, which contain fucose linked on position 4 of a GlcNAc residue; these are 8–10 times stronger inhibitors than fucose. These data demonstrate that the presence of a sialyl group does not improve the inhibitory potency of the Le^a and Le^x
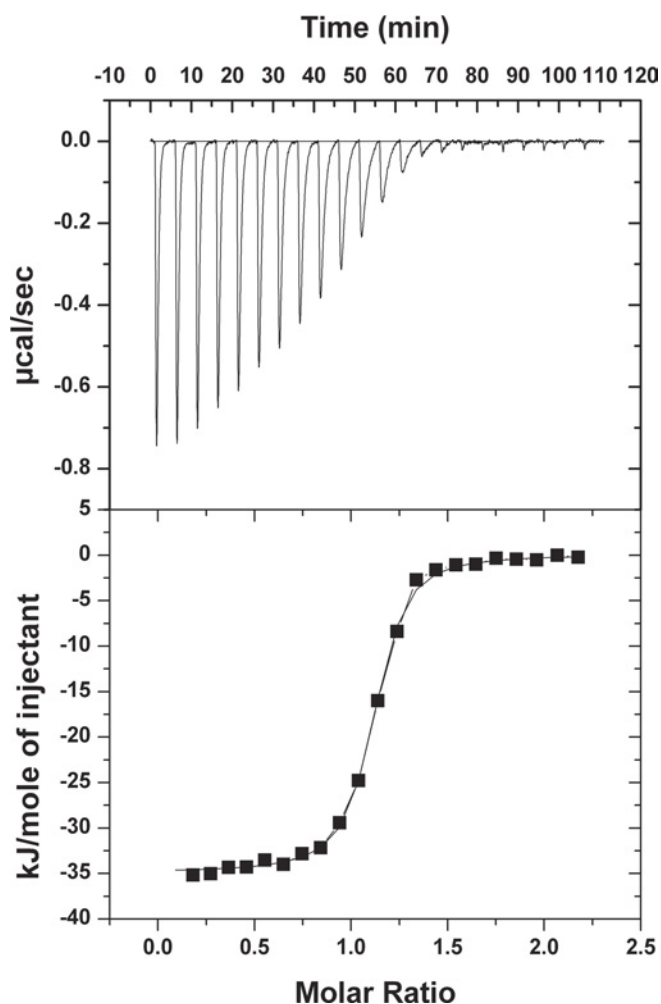
Time (min)

Figure 3   ITC analysis of the interaction of PA-IIL with Le^a

Curves are shown for Le^a (0.324 mM) binding to PA-IIL (32.7 μM) in 100 mM Tris buffer containing 0.03 mM CaCl$_2$, pH 7.5, at 25 °C. Upper panel: data were obtained from 22 automatic injections (13 μl each) of Le^a into PA-IIL in the cell. Lower panel: plot of the total heat released as a function of total ligand concentration for the titration shown in the upper panel (■). The solid line represents the best least-squares fit for the obtained data. 1 kcal = 4.184 kJ.

oligosaccharides. Moreover, the length of the oligosaccharides containing the Le^x g.a. or Le^a epitope does not modify the strength of the interaction. This indicates that only the Lewis epitope part of the oligosaccharide is responsible for the high-affinity binding to the lectin. Together, these data confirm and complete those obtained previously using different binding assays [20].

Thermodynamics of the interactions between PA-IIL and human milk oligosaccharides

In order to characterize further the interactions of the lectin with some of the most potent competitors, K_a values and thermodynamic binding parameters were analysed using ITC. A typical titration curve for the Le^a trisaccharide, the most potent ligand of PA-IIL found in the ELLA experiments described above, is shown in Figure 3. The association constant of PA-IIL–Le^a binding was 4.7×10^6 M^{-1}, some 14 times stronger than for binding of L-fucose (Table 2). The Le^x g.a. from human milk and the Le^x g.a.-containing oligosaccharides LNFP-V and LNFP-II presented K_a values 5–8 times higher than that for L-fucose. On the other hand, the affinity of the lectin for the Le^x trisaccharide was slightly lower than for fucose. These values are in agreement with the relative inhibitory potencies calculated from the ELLA experiments (Figure 2). The affinity constants described here for PA-IIL are much higher than those usually observed for lectin–oligosaccharide interactions [22].

Analyses of the different thermodynamic contributions to ligand binding indicate that the interaction is unambiguously enthalpy-driven. In all cases except one, the entropy term is small, with the $T\Delta S$ value close to 10 % of the free-energy term $-\Delta G$ (Table 2). The strong enthalpy term is not surprising, since the characteristics of fucose binding to the primary binding site are dominated by hydrogen bonding and a very unusual co-ordination to two calcium ions [20,21]. Interestingly, there is no or almost no entropy barrier for the binding of mono- or oligo-saccharides to PA-IIL. Two ligands, L-fucose and Le^a trisaccharide, present a slightly favourable entropy term, and for one ligand, Le^x, the entropy contributes almost one-third (28 %) of the binding free energy. This is unusual in protein–carbohydrate interactions, where several factors, usually attributed to flexibility of the ligand and displacement of water molecules from amphiphilic surfaces [30], generally yield an unfavourable entropy term [22]. The oligosaccharides of the Lewis series are uncommonly rigid, due to their branched structure [31,32], and this could explain the atypical favourable entropy contribution. Interestingly 3-FucLac, the glucose analogue of Le^x, binds with unfavourable entropy, which is perhaps due to a decrease in the rigidity of the trisaccharide with the absence of the N-acetyl group at position 2 (Figure 1).

Crystal structures of complexes of PA-IIL with two human milk oligosaccharides

The crystal structures of the PA-IIL–Le^a and PA-IIL–LNnFP-V complexes contain the same overall features as the PA-IIL–Fuc complex crystallized in the $P2_1$ space group and previously refined to 1.0 Å resolution [21], and in space group $P2_12_12_1$ at 1.2 Å resolution [17], showing a conserved quaternary arrangement, as well as the calcium- and fucose-binding modes (Figures 4A and 4B). The structural basis for fucose binding was

Table 2   ITC analysis for binding of PA-IIL to various oligosaccharides

Values are means ± S.D. from at least two separate titrations.

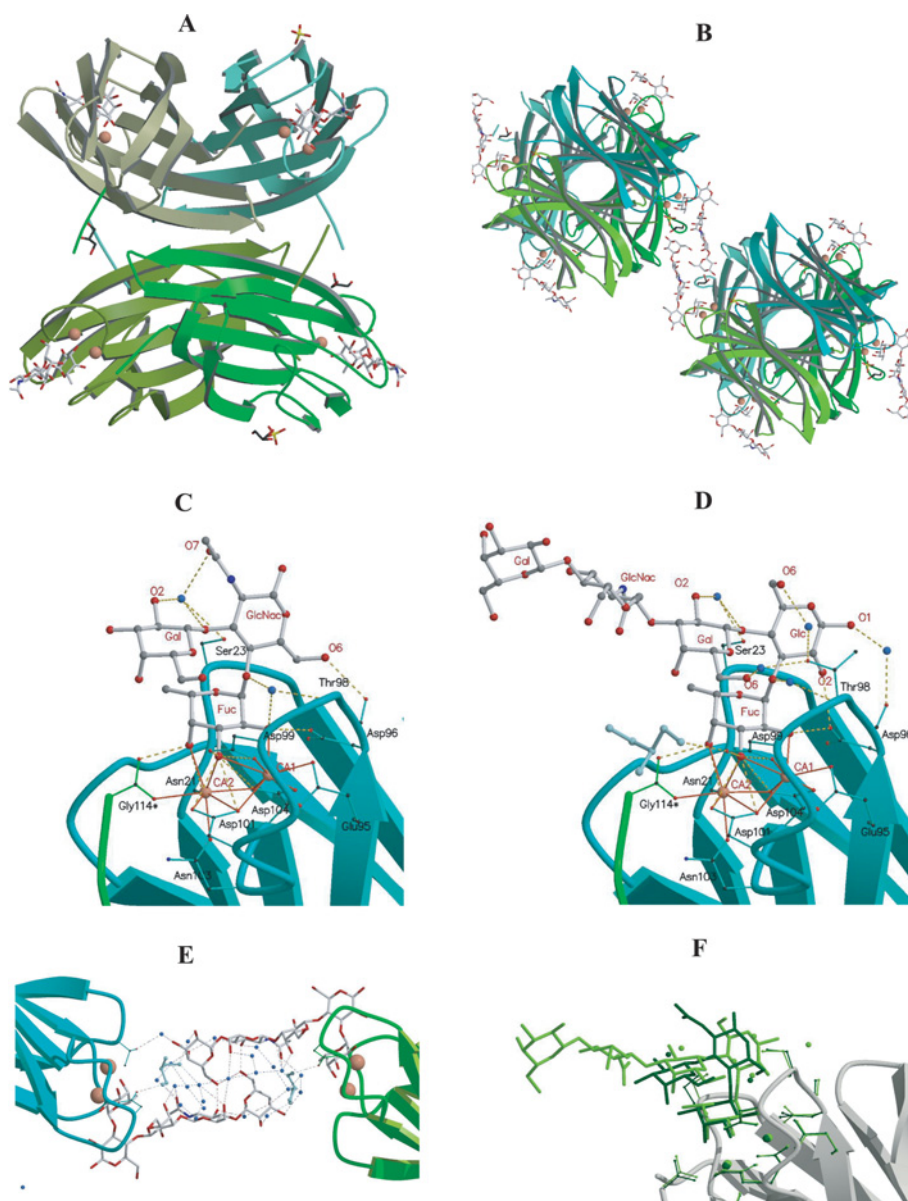| Oligosaccharide	$10^{-6} \times K_a$ (M^{-1})	n	$-\Delta G$ (kJ/mol)	$-\Delta H$ (kJ/mol)	$-T\Delta S$ (kJ/mol)
Fucose	0.34 ± 0.03	0.96 ± 0.04	31.5 ± 0.2	31.2 ± 0.1	− 0.3 ± 0.1
Le^a	4.7 ± 0.2	1.08 ± 0.01	38.06 ± 0.08	34.95 ± 0.07	− 3.11 ± 0.01
3-FucLac	2.7 ± 0.2	1.02 ± 0.01	36.7 ± 0.2	40.0 ± 0.5	3.3 ± 0.6
LNnFP-V	1.56 ± 0.04	1.02 ± 0.01	35.33 ± 0.06	35.6 ± 0.2	0.3 ± 0.3
LNFP-II	2.01 ± 0.04	0.94 ± 0.01	35.96 ± 0.05	37.8 ± 0.4	1.8 ± 0.4
Le^x	0.29 ± 0.02	0.95 ± 0.01	31.1 ± 0.2	22.3 ± 0.1	− 8.8 ± 0.3

Figure 4   Graphical representation of PA-IIL–(milk oligosaccharide) complexes

(**A**) Ribbon representation of the PA-IIL–Le^a complex tetramer, consisting of the asymmetric unit with stick representation of sugar and sulphate and cpk representation of the calcium ions. (**B**) Same representation for the structure of the PA-IIL–LNnFP-V complex, showing the interaction between two tetramers (orientation orthogonal to that of **A**). (**C**) Interactions of PA-IIL with calcium ions and Le^a. Co-ordination contacts are indicated by orange solid lines and hydrogen bonds by green dashed lines. (**D**) Same representation for the interaction of PA-IIL with calcium ions and LNnFP-V. (**E**) Interaction between two pentasaccharides in the PA-IIL–LNnFP-V complex. Hydrogen bonds are represented by dotted lines. (**F**) Superimposition of the binding sites of the PA-IIL–Le^a and PA-IIL–LNnFP-V complexes.

discussed in detail previously [21]. There are few structural data on fucose-binding lectins at the present time; complexes of fucose with *Ulex europaeus* lectin I [33], eel lectin [34], fungal *Aleuria aurantia* lectin [35] and mutated mannan-binding protein-A [36] interestingly display completely different structural features, and no comparisons can be made.

Of special interest is the analysis of the conformations of the two oligosaccharides that are reported here for the first time in the crystalline state, together with their interactions with the protein receptor. There are no significant differences among the four monomers of PA-IIL–Le^a present in the asymmetric unit. Analysis of the mode of binding of Le^a by PA-IIL reveals a large number of contacts between the sugar and the protein (Figure 4C). All three of the monosaccharides interact with the protein surface

either directly (hydrogen bonding and co-ordination of calcium) or indirectly through bridging water molecules (Table 3). In addition to the nine direct hydrogen bonds between the fucose and the protein described previously, the GlcNAc residue establishes a hydrogen bond between its O-6 atom and the main-chain carbonyl group of Asp-96. Two water molecules play an important bridging role in the interaction: one bridges O-1 and O-2 of fucose to the amide nitrogen of Thr-98, whereas the other bridges the Gal residue (O-2 and O-1) to the side chain of Ser-23. Hydrophobic contacts are very limited and only involve the methyl group of fucose with that of Thr-145. Due to its branched structure, Le^a has been described as a rigid trisaccharide in NMR and modelling studies [31,32]. Indeed, our results show that the conformation adopted by Le^a in the binding site is similar to that predicted by

Table 3   Contact of interest in the binding site of PA-IIL–oligosaccharide complexes

Distances (Å) are averaged over the four proteins in the asymmetric unit, and S.D.s on the last digit are given in parentheses. Wat_1 and Wat_2 are the water molecules present in the carbohydrate-binding site (coloured blue in Figures 4A and 4B). The asterisk in Gly-114* OXT indicates that this residue belongs to the neighbouring monomer. Bridging is indicated by superscript numbers as follows: [1]bridged to Thr-98 N, [2]bridged to Thr-98 N and Asp-99 N, [3]bridged to Ser-23 OG, [4]bridged to Asp-96 O, [5]bridged to Thr-98 OG1.

PA-IIL–Le[a] complex			PA-IIL–LNnFP-V complex		
Interacting species			Interacting species		
PA-IIL	Le[a]	Distance (Å)	PA-IIL	LNnFP-V	Distance (Å)
Ca-1	O-2 Fuc	2.50 (3)	Ca-1	O-2 Fuc	2.45 (1)
Ca-1	O-3 Fuc	2.53 (5)	Ca-1	O-3 Fuc	2.47 (1)
Ca-2	O-3 Fuc	2.50 (3)	Ca-2	O-3 Fuc	2.47 (1)
Ca_2	O-4 Fuc	2.47 (2)	Ca_2	O-4 Fuc	2.49 (1)
Wat_1[1]	O-1 Fuc	2.96 (9)	Wat_1[2]	O-1 Fuc	2.96 (4)
Wat_1[1]	O-2 Fuc	3.1 (1)			
Asp-96 OD1	O-2 Fuc	2.64 (2)	Asp-96 OD1	O-2 Fuc	2.7 (1)
Asp-99 OD1	O-3 Fuc	2.98 (7)	Asp-99 OD1	O-3 Fuc	2.97 (2)
Asp-99 OD2	O-3 Fuc	2.48 (1)	Asp-99 OD2	O-3 Fuc	2.55
Asp-101 OD1	O-3 Fuc	2.94 (1)	Asp-101 OD1	O-3 Fuc	2.97 (1)
Asp-101 OD2	O-3 Fuc	2.94 (1)	Asp-101 OD2	O-3 Fuc	2.98 (1)
Asp-104 OD2	O-3 Fuc	3.07 (3)	Asp-104 OD2	O-3 Fuc	3.00 (1)
Asn-21 O	O-4 Fuc	2.98 (4)	Asn-21 O	O-4 Fuc	3.01 (4)
Gly-114* OXT	O-4 Fuc	2.55 (3)	Gly-114* OXT	O-4 Fuc	2.56 (1)
Ser-23 N	O-5 Fuc	3.03 (3)	Ser-23 N	O-5 Fuc	2.96 (1)
Thr-45 CG2	C-6 Fuc	4.10 (5)	Thr-45 CG2	C-6 Fuc	4.1 (1)
Asp-96 O	O-6 GlcNAc	2.7 (1)	Asp-96 OD1	O-2 Glc	2.74 (3)
Wat_2[3]	O-7 GlcNAc	3.1 (2)	Wat_3[4]	O-1 Glc	2.4 (1)
			Wat_4[5]	O-6 Glc	3.0 (1)
Wat_2	O-1 Gal	3.08 (2)	Wat_2	O-2 Gal	2.72 (2)
Wat_2	O-2 Gal	2.72 (3)	Wat_1	O-6 Gal	2.71 (3)
			Wat_5[4]	O-6 Gal	3.1 (4)

Table 4   Torsion angles of interest of Le[a] in the binding site of PA-IIL

Mol A to Mol D correspond to the four different monomers present in the asymmetric unit. Φ is defined as $\Theta(O\text{-}5\text{–}C\text{-}1\text{–}O\text{-}1\text{–}C\text{-}x)$; Ψ is defined as $\Theta[C\text{-}1\text{–}O\text{-}1\text{–}C\text{-}x\text{–}C\text{-}(x+1)]$.

	Mol A	Mol B	Mol C	Mol D
αFuc1-4βGlcNac				
Φ	− 66.9	− 72.8	− 75	− 77.1
Ψ	− 105.2	− 100.6	− 104.9	− 105.4
βGal1-3βGlcNAc				
Φ	− 65.7	− 71	− 62.3	− 78.3
Ψ	134.7	130.5	128.6	144.5

A

B

Figure 5   Initial sigma-weighted F_o–F_c electron density map

(**A**) The map has been contoured at 1σ around the trisaccharide in the PA-IIL–Le[a] complex calculated after molecular replacement and first cycle of refinement without ligand and water. (**B**) Same representation for the pentasaccharide in the PA-IIL–LNnFP-V complex after phasing with Acorn. The final positions of the oligosaccharide and calcium in the model have been superimposed as thin lines for comparison.

those earlier studies, confirming the rigidity of the trisaccharide. Torsion angles of interest are listed in Table 4.

Among the four independent molecules of the PA-IIL–LNnFP-V complex, clear electron density can be observed for two complete pentasaccharides (Figure 5), whereas only a tetrasaccharide and a trisaccharide can be located for the two remaining sites. The fact that two of the oligosaccharides can be completely visualized is due the rigidity of their linear part resulting from fortuitous crystal packing that generates extensive contacts between two adjacent sugars centred around a pseudo two-fold axis of symmetry (Figure 4E). It is this interaction that allows the very-high-resolution structure of milk pentasaccharide to be described here for the first time. The protein-binding site, together with the calcium ions and fucose moiety, are identical with those described previously. Additional interactions with the protein surface are established by the glucose and galactose residues of the Le[x] g.a. moiety (Figure 4D and Table 3). The glucose establishes a direct hydrogen bond between its hydroxy group at position 2 and the side chain of Asp-96. In addition, five interactions are mediated by a water molecule, involving O-1 of fucose, O-1 and O-6 of glucose, and O-1, O-2 and O-6 of galactose. Hydrophobic interactions are observed for the methyl group of fucose, but also for C-6 of galactose, which interacts with the carbon of a glycerol molecule located at the protein surface. The other part of the pentasaccharide, i.e. the βGlc1-4βGlcNAc linked to position 3 of galactose, does not interact with the protein surface, but instead is involved in extensive interactions with the neighbouring carbohydrate in the crystal lattice (Figure 4E).

The conformations of the pentasaccharide correspond to a low-energy minimum of each glycosidic linkage, as established previously by conformational analysis studies [32]. The 3-FucLac moiety (Le[x] g.a.) is the most rigid part, and it adopts a conformation with glycosidic linkage orientations similar to those observed in the crystal structure of hydrated Le[x] [37] (Table 5).

DISCUSSION

The binding of carbohydrate ligands to the fucose-binding lectin of *P. aeruginosa* presents some particular features that are not commonly observed in protein–carbohydrate interactions. Its

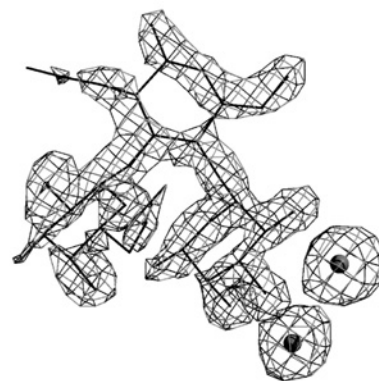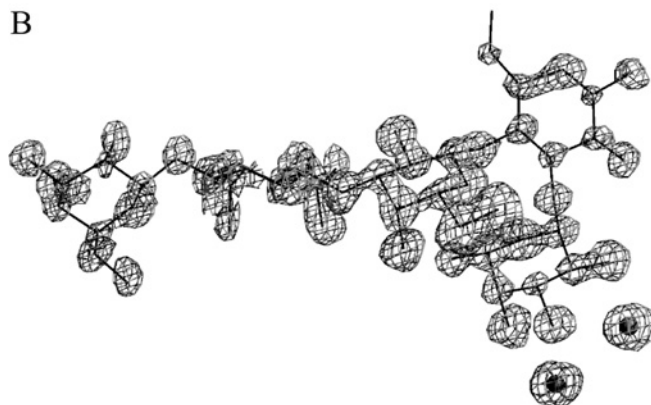**Table 5   Torsion angles of interest of LNnFP-V in the binding site of PA-IIL**

Mol A to Mol D correspond to the four different monomers present in the asymmetric unit. Φ is defined as Θ(O-5–C-1–O-1-C-x); Ψ is defined as Θ[C-1–O-1–C-x-C-(x + 1)]. For Le^x, torsion angles are given for αFuc1-3GlcNAc and βGal1-4GlcNAc linkages in the two independent molecules of hydrated Le^x crystal.

	Mol A	Mol B	Mol B	Mol D	Le^x
αFuc1-3βGlc					
Φ	− 76.4	− 75.5	− 78.9	− 77.5	− 72.5/− 76.7
Ψ	138.6	141.2	142.3	140.6	139.2/139.0
βGal1-4βGlc					
Φ	− 70.3	− 69.7	− 68.3	− 69.3	− 80.0/− 70.5
Ψ	− 104.1	− 104.2	− 101.4	− 104.0	− 104.6/− 107.7
βGlcNAc1-3βGal					
Φ	− 91.8	− 84.6		− 87.7	
Ψ	84.2	119.4		120.1	
βGal1-4βGlcNAc					
Φ		− 71.3		− 76.9	
Ψ		− 112.2		− 111.8	

monosaccharide binding has been characterized previously: the low specificity was rationalized in terms of the structural features required to co-ordinate the two calcium ions [17], whereas the high affinity has also been attributed to the presence of cations with charge delocalization [21]. A special feature is the favourable, albeit very weak, entropy that has been observed for fucose binding that could be generated by the release of three tightly bound water molecules (observed in the crystal structure of the unliganded lectin [17]) that are replaced by fucose hydroxy groups in the complex.

When looking at oligosaccharide binding, and more particularly at human milk oligosaccharides that can play a role in early-stage colonization, the specificity of PA-IIL is limited to those oligosaccharides with fucose linked to position 4 of GlcNAc, and not to position 3. This is rationalized by the two high-resolution crystal structures presented here. In Le^a, the Fuc1-4GlcNAc linkage positions O-6 of GlcNAc in a favourable location to create an additional hydrogen bond with the protein backbone (Figure 4C). For the Le^x trisaccharide, the Fuc1-3GlcNAc linkage would locate the N-acetyl group to the same position, therefore creating steric conflicts; this will result in a deformation of the trisaccharide, weaker binding and, more particularly, as observed in ITC, a large decrease in the enthalpy term. In Le^x g.a., the N-acetyl group at position 2 is replaced by a hydroxy group that makes a hydrogen bond to the protein (Figure 4D). Superimposition of the two binding sites (Figure 4F) shows that Le^x g.a. adopts a slightly different orientation than Le^a in the binding site.

The specificity range established by ELLA experiments gives same order of ligand affinity as the titration study in solution, demonstrating that the lectin is fully active when fixed on the surface. The microcalorimetry study confirmed that the highest-affinity ligand was the Le^a trisaccharide, and that it binds with very high enthalpy contribution ($\Delta H = - 35$ kJ/mol) and slightly favourable entropy ($- T \Delta S = - 3$ kJ/mol). Interestingly, the Le^x g.a. presents an unfavourable entropy contribution. This could be due either to the absence of the N-acetyl group that brings higher flexibility to the adjacent linkage, or to the fact that the binding involves three more bridging water molecules, immobilization of which generates an entropy penalty.

The large variety of fucosylated oligosaccharides that are present in human milk (> 100) may represent an adapted and specific response to block a large number of pathogens. For example, *C. jejuni* is specifically blocked by H(O) antigen (αFuc1-2βGal1-4GlcNAc) [11] whereas *H. pylori* is blocked by Lewis b epitope (αFuc1-2βGal1–3[αFuc1-4]GlcNAc) [13]. The presence of the three different fucosyl epitopes in milk, i.e. αFuc1-2βGal, αFuc1-3Glc/GlcNAc and αFuc1-4GlcNAc, is genetically determined primarily by the action of a Lewis gene coding for an α1,3/4-fucosyltransferase and a secretor gene coding for an α1,2-fucosyltransferase [38]. In the European population, as a consequence of polymorphisms yielding inactive or partially active enzymes, approx. 70 % of women will have α1,2-, α1,3- and α1,4-linked fucosyl residues in their milk. Fucosyl residues linked α1,2 and α1,4 will be absent from 20 % and 10 % of the population respectively. A clear relationship has been established between maternal genotype and the risk of diarrhoea in their infants [39]. The *P. aeruginosa* lectin is blocked by α1,4GlcNAc- but also by α1,3Glc-linked fucosyl residues that are present in the milk of all women. It is therefore most interesting that these two epitopes are the ones that present the highest affinity found to date for the soluble lectin of *Pseudomonas aeruginosa*.

REFERENCES

1 Beachey, E. H. (1981) Bacterial adherence: adhesin-receptor interactions mediating the attachment of bacteria to mucosal surface. J. Infect. Dis. **143**, 325–345

2 Hahn, H. P. (1997) The type-4 pilus is the major virulence-associated adhesin of *Pseudomonas aeruginosa*. Gene **192**, 99–108

3 Arora, S. K., Ritchings, B. W., Almira, E. C., Lory, S. and Ramphal, R. (1998) The *Pseudomonas aeruginosa* flagellar cap protein, FliD, is responsible for mucin adhesion. Infect. Immun. **66**, 1000–1007

4 Gilboa-Garber, N. (1982) *Pseudomonas aeruginosa* lectins. Methods Enzymol. **83**, 378–385

5 Mysore, J. V., Wigginton, T., Simon, P. M., Zopf, D., Heman-Ackah, L. M. and Dubois, A. (1999) Treatment of *Helicobacter pylori* infection in rhesus monkeys using a novel antiadhesion compound. Gastroenterology **117**, 1316–1325

6 Tong, H. H., McIver, M. A., Fisher, L. M. and DeMaria, T. F. (1999) Effect of lacto-N-neotetraose, asialoganglioside-GM1 and neuraminidase on adherence of otitis media-associated serotypes of *Streptococcus pneumoniae* to chinchilla tracheal epithelium. Microb. Pathog. **26**, 111–119

7 Sharon, N. and Ofek, I. (2000) Safe as mother's milk: carbohydrates as future anti-adhesion drugs for bacterial diseases. Glycoconj. J. **17**, 659–664

8 Chaturvedi, P., Warren, C. D., Altaye, M., Morrow, A. L., Ruiz-Palacios, G., Pickering, L. K. and Newburg, D. S. (2001) Fucosylated human milk oligosaccharides vary between individuals and over the course of lactation. Glycobiology **11**, 365–372

9 Kunz, C., Rudloff, S., Baier, W., Klein, N. and Strobel, S. (2000) Oligosaccharides in human milk: structural, functional, and metabolic aspects. Annu. Rev. Nutr. **20**, 699–722

10 Newburg, D. S., Pickering, L. K., McCluer, R. H. and Cleary, T. G. (1990) Fucosylated oligosaccharides of human milk protect suckling mice from heat-stabile enterotoxin of Escherichia coli. J. Infect. Dis. **162**, 1075–1080

11 Ruiz-Palacios, G. M., Cervantes, L. E., Ramos, P., Chavez-Munguia, B. and Newburg, D. S. (2003) *Campylobacter jejuni* binds intestinal H(O) antigen (Fuc alpha 1, 2Gal beta 1, 4GlcNAc), and fucosyloligosaccharides of human milk inhibit its binding and infection. J. Biol. Chem. **278**, 14112–14120

12 Huang, P., Farkas, T., Marionneau, S., Zhong, W., Ruvoen-Clouet, N., Morrow, A. L., Altaye, M., Pickering, L. K., Newburg, D. S., Le Pendu, J. and Jiang, X. (2003) Noroviruses bind to human ABO, Lewis, and secretor histo-blood group antigens: identification of 4 distinct strain-specific patterns. J. Infect. Dis. **188**, 19–31

13 Xu, H. T., Zhao, Y. F., Lian, Z. X., Fan, B. L., Zhao, Z. H., Yu, S. Y., Dai, Y. P., Wang, L. L., Niu, H. L., Li, N. et al. (2004) Effects of fucosylated milk of goat and mouse on Helicobacter pylori binding to Lewis b antigen. World J. Gastroenterol. **10**, 2063–2066

14 Olson, B., Weinstein, R. A., Nathan, C., Chamberlin, W. and Kabins, S. A. (1984) Epidemiology of endemic *Pseudomonas aeruginosa*: why infection control efforts have failed. J. Infect. Dis. **150**, 808–816

15 Ohara, T. and Itoh, K. (2003) Significance of *Pseudomonas aeruginosa* colonization of the gastrointestinal tract. Intern. Med. **42**, 1072–1076

16   Gilboa-Garber, N., Katcoff, D. J. and Garber, N. C. (2000) Identification and characterization of *Pseudomonas aeruginosa* PA-IIL lectin gene and protein compared to PA-IL. FEMS Immunol. Med. Microbiol. **29**, 53–57

17   Loris, R., Tielker, D., Jaeger, K.-E. and Wyns, L. (2003) Structural basis of carbohydrate recognition by the lectin LecB from *Pseudomonas aeruginosa*. J. Mol. Biol. **331**, 861–870

18   Winzer, K., Falconer, C., Garber, N. C., Diggle, S. P., Camara, M. and Williams, P. (2000) The *Pseudomonas aeruginosa lectins* PA-IL and PA-IIL are controlled by quorum sensing and by RpoS. J. Bacteriol. **182**, 6401–6411

19   Lesman-Movshovich, E., Lerrer, B. and Gilboa-Garber, N. (2003) Blocking of *Pseudomonas aeruginosa* lectins by human milk glycans. Can. J. Microbiol. **49**, 230–235

20   Mitchell, E., Houles, C., Sudakevitz, D., Wimmerova, M., Gautier, C., Pérez, S., Wu, A. M., Gilboa-Garber, N. and Imberty, A. (2002) Structural basis for oligosaccharide-mediated adhesion of *Pseudomonas aeruginosa* in the lungs of cystic fibrosis patients. Nat. Struct. Biol. **9**, 918–921

21   Mitchell, E. P., Sabin, S., Šnajdrová, L., Budová, M., Perret, S., Gautier, C., Hofr, C., Gilboa-Garber, N., Koca, J., Wimmerová, M. and Imberty, A. (2005) High affinity fucose binding of *Pseudomonas aeruginosa* lectin PA-IIL: 1.0 Å resolution crystal structure of the complex combined with thermodynamics and computational chemistry approaches. Proteins: Struct. Funct. Bioinform. **58**, 735–748

22   Dam, T. K. and Brewer, C. F. (2002) Thermodynamic studies of lectin-carbohydrate interactions by isothermal titration calorimetry. Chem. Rev. **102**, 387–429

23   Dumon, C., Priem, B., Martin, S. L., Heyraud, A., Bosso, C. and Samain, E. (2001) *In vivo* fucosylation of lacto-N-neotetraose and lacto-N-neohexaose by heterologous expression of *Helicobacter pylori* alpha-1,3 fucosyltransferase in engineered *Escherichia coli*. Glycoconj. J. **18**, 465–474

24   Leslie, A. G. W. (1992) Recent changes to the MOSFLM package for processing film and image plate data. Joint CCP4 + ESF-EAMCB Newsletter on Protein Crystallography **26**

25   Computational Collaborative Project Number4 (1994) The CCP4 suite: programs for protein crystallography. Acta Crystallogr. D Biol. Crystallogr. **50**, 760–763

26   Cowtan, K. D. and Zhang, K. Y. (1999) Density modification for macromolecular phase improvement. Prog. Biophys. Mol. Biol. **72**, 245–270

27   Perrakis, A., Morris, R. and Lamzin, V. S. (1999) Automated protein model building combined with iterative structure refinement. Nat. Struct. Biol. **6**, 458–463

28   Jones, T. A., Zou, J. Y., Cowan, S. W. and Kjeldgaard, M. (1991) Improved methods for building protein models in electron density maps and the location of errors in these models. Acta Crystallogr. A **47**, 110–119

29   Murshudov, G. N., Vagin, A. A. and Dodson, E. J. (1997) Refinement of macromolecular structures by the maximum-likelihood method. Acta Crystallogr. D Biol. Crystallogr. **53**, 240–255

30   Lemieux, R. U., Delbaere, L. T., Beierbeck, H. and Spohr, U. (1991) Involvement of water in host-guest interactions. Ciba Found. Symp. **158**, 231–245

31   Lemieux, R. U., Bock, K., Delbaere, L. T. J., Koto, S. and Rao, V. S. R. (1980) The conformations of oligosaccharides related to the ABH and Lewis human blood group determinants. Can. J. Chem. **58**, 631–653

32   Imberty, A., Mikros, E., Koca, J., Mollicone, R., Oriol, R. and Pérez, S. (1995) Computer simulation of histo-blood group oligosaccharides. Energy maps of all constituting disaccharides and potential energy surfaces of 14 ABH and Lewis carbohydrate antigens. Glycoconj. J. **12**, 331–349

33   Audette, G. F., Olson, D. J. H., Ross, A. R. S., Quail, J. W. and Delbaere, L. T. (2002) Examination of the structural basis for O(H) blood group specificity by *Ulex europaeus* lectin I. Can. J. Chem. **80**, 1010–1021

34   Bianchet, M. A., Odom, E. W., Vasta, G. R. and Amzel, L. M. (2002) A novel fucose recognition fold involved in innate immunity. Nat. Struct. Biol. **9**, 628–634

35   Wimmerova, M., Mitchell, E., Sanchez, J. F., Gautier, C. and Imberty, A. (2003) Crystal structure of fungal lectin: Six-bladed β-propeller fold and novel recognition mode for *Aleuria aurantia* lectin. J. Biol. Chem. **278**, 27059–27067

36   Ng, K. K., Drickamer, K. and Weis, W. I. (1996) Structural analysis of monosaccharide recognition by rat liver mannose-binding protein. J. Biol. Chem. **271**, 663–674

37   Pérez, S., Mouhous-Riou, N., Nifant'ev, N. E., Tsvetkov, Y. E., Bachet, B. and Imberty, A. (1996) Crystal and molecular structure of a histo-blood group antigen involved in cell adhesion: the Lewis x trisaccharide. Glycobiology **6**, 537–542

38   Henry, S., Oriol, R. and Samuelsson, B. (1995) Lewis histo-blood group system and associated secretory phenotypes. Vox Sang. **69**, 166–182

39   Newburg, D. S., Ruiz-Palacios, G. M., Altaye, M., Chaturvedi, P., Meinzen-Derr, J., Guerrero, M. L. and Morrow, A. L. (2004) Innate protection conferred by fucosylated oligosaccharides of human milk against diarrhea in breastfed infants. Glycobiology **14**, 253–263